

BCSJ Award Article

Selective Recognition of Trp- and Tyr-Rich Oligopeptides by Self-Assembled Coordination Hosts

Shohei Tashiro and Makoto Fujita*

Department of Applied Chemistry, School of Engineering, The University of Tokyo and CREST, Japan Science and Technology Agency (JST), 7-3-1 Hongo, Bunkyo-ku, Tokyo 113-8656

Received December 13, 2005; E-mail: mfujita@appchem.t.u-tokyo.ac.jp

A coordination host recognized various aromatic peptides containing Trp and Tyr residues in a highly sequence-selective fashion. For example, two similar hexa-peptides, Ac-Ser-Gly-Ala-Trp-Trp-Ala-NH_2 and Ac-Ala-Trp-Trp-Ala-Gly-Ser-NH_2, were selectively discriminated by the restricted inner space of coordination cages. We also demonstrated that the charged peptides were efficiently discriminated by the cage owing to the highly cationic property of the cage (12+). Furthermore, the cages selectively discriminated two similar peptides, Ac-Ala-Trp-Trp-NH_2 and Ac-Ala-Tyr-Tyr-NH_2, because of differences in the strength of charge-transfer interaction between the cage and the electron-rich aromatic residues. This selectivity was controlled by modulating the solution pH. The colorization of the aromatic peptide solutions by charge-transfer interaction could also be applicable to the naked-eye recognition of three aromatic residues, Trp, Tyr, and Phe.

Peptide recognition is an essential process in biological events, such as protein–protein interaction, hormone–receptor interaction, and cell–cell adhesion.[1] In peptide recognition by synthetic receptors, it is particularly important to recognize the sequence of peptides because sequence-selective peptide recognition can be applied to the site-specific recognition of the protein surface, which leads to control of protein–protein and protein–substrate interactions.[2] Recently, for the site-specific recognition of protein surfaces, a number of artificial peptide receptors have been designed. In general, the sequence-selective recognition of oligopeptides is accomplished by linking two or more binding sites of synthetic receptors.[3] An interesting example is Hamilton's well-designed receptors that recognize peptide secondary structures such as the α-helix as well as a protein surface.[4]

It is known that protein surfaces mediating protein–protein interactions are abundant in aromatic residues such as Tyr and Trp.[5] Those aromatic residues are especially localized in the antigen binding sites of antibodies, which are called complementarity determining regions (CDR).[6] Thus, sequence-selective recognition of aromatic residues is particularly important to control the protein surface interactions. Cyclodextrin, which is one of the useful aromatic peptide receptors, can bind only one aromatic side chain within its relatively small cavity. For aromatic oligopeptide recognition, two or more cyclodextrins should be linked by covalent bonds.[7]

Recently, we have shown that nanometer-sized hollow compounds are self-assembled from simple organic ligands and transition metals such as palladium or platinum ions.[8] These large hollow compounds can accommodate several organic molecules within a large hydrophobic cavity in water.[9] Furthermore, the single binding pocket of the coordination cage exhibited sequence-selective recognition of tripeptide possessing Trp residues via the full encapsulation of the tripeptide.[10] Here, we describe how coordination cages are utilized as good aromatic peptide receptors with high selectivity and affinity. The cages discriminate oligopeptides possessing analogous sequences through accommodation in the restricted cavity. The highly cationic property of the cages is also applicable to the selective recognition of charged residues, where the selectivity can be controlled by the pH condition. Furthermore, we demonstrate the naked-eye recognition of aromatic peptides from the change of solution color, which is attributed to charge-transfer interaction between the cage and aromatic peptides.

Results and Discussion

Nature and Recognition Ability of Platinum Cage 1. The self-assembled platinum cage **1** used in this report has several advantages for molecular recognition. 1) The inner space surrounded by four organic ligands can accommodate aromatic molecules through π–π and hydrophobic interactions. 2) Electron-rich molecules are bound through charge-transfer interaction with triazine ligands, which have an electron-deficient property due to electron-withdrawing by metal ions. 3) The restricted inner space can recognize the size and shape of guest molecules. 4) Since cage **1** is highly cationic (12+), anionic molecules show a higher affinity than neutral and cationic molecules. 5) The platinum cage **1** has substantial stability

Published on the web June 6, 2006; doi:10.1246/bcsj.79.833

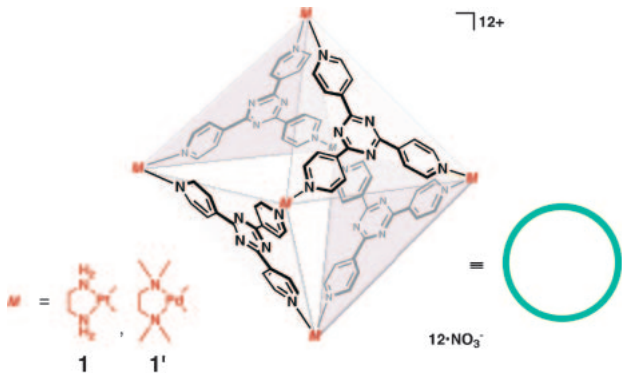

Scheme 1.

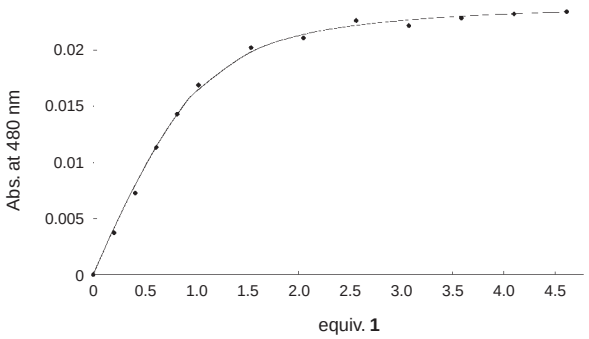

Fig. 1. UV–vis titration curve of peptide **2** with cage **1**, monitored charge-transfer band at 480 nm. [**2**] = 40 μM in 5 mM acetate buffer (pH 4.8) at 20 °C.

for basic and acidic conditions compared with the acid and base sensitive palladium cage **1′** (Scheme 1).[11]

The platinum cage **1** bound Ac-Trp-Trp-Ala-NH_2 (**2**) very strongly and selectively in water as described in a previous report.[10] The complex **1·2** was easily prepared by mixing a solution of **1** and **2** at room temperature for a few minutes. The solution of complex **1·2** exhibited an orange color that was ascribed to charge transfer from indole rings to the electron-deficient triazine ligands of **1**. By monitoring this charge-transfer absorption upon the addition of **1** into **2**, the association constant of **1·2** was determined (Fig. 1). From a nonlinear curve-fitting procedure, the K_a of **1·2** was estimated to be $1.5 \times 10^5\ M^{-1}$, which was slightly smaller than the case of the palladium cage **1′** ($K_a > 10^6\ M^{-1}$).[10] This seemed to be a subtle difference of cavity size due to the variation of metal ions (Pt(II) vs Pd(II)) and end-capped groups (ethylenediamine vs *N*,*N*,*N*′,*N*′-tetramethylethylenediamine). In a similar way to the Pd(II)-cage **1′**, the Pt(II)-cage **1** dominantly recognized **2** and Ac-Trp-Ala-Trp-NH_2 (**3**) over Ac-Ala-Trp-Trp-NH_2 (**4**) and Ac-Trp-Trp-Gly-NH_2 (**5**) (Table 1). The geometry of **1·2** was not different from that of **1′·2** because ^{1}H NMR chemical shifts of **1·2** and **1′·2** were almost the same (Supporting Information). The importance of the presence of an aromatic residue(s) was proven by the lack of affinity of an aliphatic tripeptide, Ac-Gly-Gly-Ala-NH_2 (**6**) with the cage.

Selective and Site-Specific Recognition of Hexapeptides. We examined the selective recognition of not only tripeptides, but also longer peptides by using the steric effect of cage **1**. Hexapeptide, Ac-Ser-Gly-Ala-**Trp**-**Trp**-**Ala**-NH_2 (**7**), possessing an additional Ser-Gly-Ala sequence at the N-terminal of **2**, was bound in **1** with high affinity ($K_a > 10^5\ M^{-1}$). However, Ac-Ala-**Trp**-**Trp**-**Ala**-Gly-Ser-NH_2 (**8**), having additional sequences at both terminals of **2**, showed poorer affinity than **7** ($K_a = 7.2 \times 10^4\ M^{-1}$). Namely, cage **1** discriminated between two similar hexapeptides consisting of the same residues in different sequences (Table 2). This selectivity is explained by the fact that the stable conformation of **1·2** is disturbed by steric repulsion between the cage and the elongated sequence at the C-terminal. The crystal structure of complex **1′·2** shows that the C-terminal of **2** is more deeply involved in the cavity than the N-terminal (Fig. 2).[10] Namely, cage **1** can recognize long polypeptide chains with a Trp-Trp-Ala sequence at the C-terminal (with high affinity of $>10^5\ M^{-1}$), such as the peptide **7**.

Interestingly, even for the hexapeptide **8**, which contains a Trp-Trp-Ala sequence at the middle, the Trp-Trp-Ala portion was recognized to form a pseudo-rotaxane structure with cage **1** or **1′**. Thus, in the NMR analysis of the **1′·8** complex, signals of the Trp2-Trp3-Ala4 sequence and Gly5 were significantly up-field shifted, whereas other residues, Ala1 and Ser6, exhibited a slight down-field shift (Fig. 3). From comparison between NMR chemical shifts of **1·8** and **1′·8**, the peptide **8** was accommodated within the cavity of the Pt(II)-cage **1** in

Table 1. Association Constants of **1** with Tripeptides in Water

Peptides	K_a/M^{-1} a)
Ac-**Trp**-**Trp**-Ala-NH_2 (**2**)	$1.5\ (\pm 4.9) \times 10^5$
Ac-**Trp**-Ala-**Trp**-NH_2 (**3**)	$1.1\ (\pm 0.4) \times 10^5$
Ac-Ala-**Trp**-**Trp**-NH_2 (**4**)	$3.7\ (\pm 0.6) \times 10^4$
Ac-**Trp**-**Trp**-Gly-NH_2 (**5**)	$6.6\ (\pm 0.8) \times 10^4$
Ac-Gly-Gly-Ala-NH_2 (**6**)	no binding

a) Measured by UV–vis titration at 20 °C in 5 mM acetate buffer (pH 4.8).

Table 2. Association Constants of **1** with Hexapeptides in Water

Peptides	K_a/M^{-1} a)
Ac-Ser-Gly-Ala-**Trp**-**Trp**-Ala-NH_2 (**7**)	$>10^5$
Ac-Ala-**Trp**-**Trp**-Ala-Gly-Ser-NH_2 (**8**)	$7.2\ (\pm 1.9) \times 10^4$

a) Measured by UV–vis titration at 20 °C in 5 mM acetate buffer (pH 4.8).

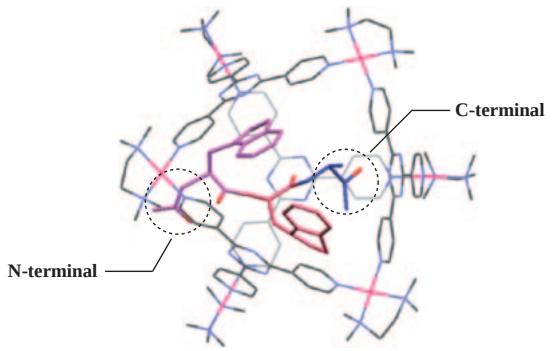

Fig. 2. Crystal structure of the **1′·2** complex.[10] The N-terminal and C-terminal are emphasized.

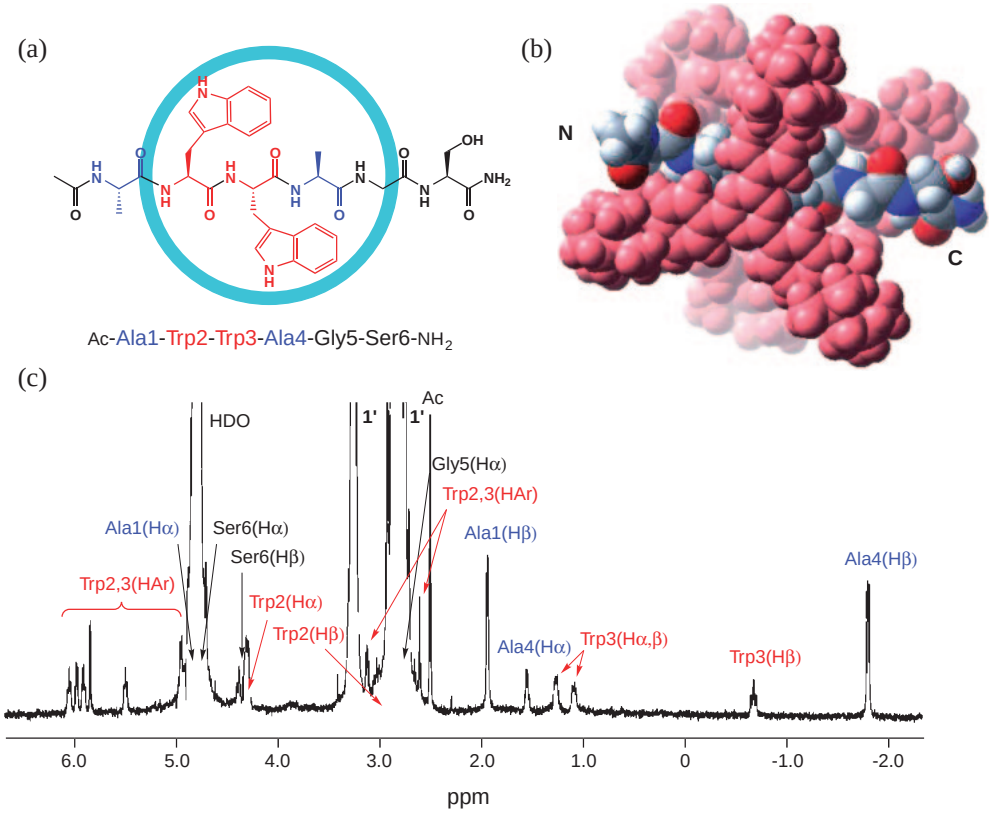

Fig. 3. (a) Schematic representation of complex **1′·8**. (b) Molecular modeling of complex **1′·8** (cage **1′** is pale red). (c) ^{1}H NMR of **1′·8** in D_2O (500 MHz, 2 mM).

Table 3. Association Constants of **1** with Peptides in Water

Peptides	K_a/M^{-1} a)	
	pH 4.8 (Acetate buffer)	pH 9.0 (Borate buffer)
Ac-**Trp**-**Trp**-Ala-NH_2 (**2**)	1.5 (±4.9) × 10^5	1.9 (±3.4) × 10^5
H-**Trp**-**Trp**-Ala-OH (**9**)	4.7 (±1.6) × 10^4	>10^6
Ac-Ala-**Trp**-**Trp**-Ala-Gly-Ser-NH_2 (**8**)	7.2 (±1.9) × 10^4	9.5 (±1.5) × 10^4
Ac-Ala-**Trp**-**Trp**-Ala-Gly-Lys-NH_2 (**10**)	<10^3	2.0 (±0.3) × 10^4
Ac-Ala-**Trp**-**Trp**-Ala-Gly-Glu-NH_2 (**11**)	2.4 (±0.4) × 10^5 b)	>10^6

a) Measured by UV–vis titration at 20 °C in 5 mM buffer solution. b) Measured in 5 mM phosphate buffer solution (pH 2.6).

the same manner as the Pd(II)-cage **1′**. This suggests that the cages can bind the Trp-Trp-Ala sequence at any position of a long peptide chain with moderate affinity (>10^4 M^{-1}).

Electrostatic Repulsion or Attraction between the Cage and Peptides. Due to the highly cationic property of cage **1** (12+), charged peptides were strictly discriminated by electrostatic attraction and repulsion in various pH conditions. For example, the binding affinity of the non-protected tripeptide H-Trp-Trp-Ala-OH (**9**) was dramatically affected by pH. In an acetate buffer (pH 4.8), **9** showed poorer affinity than **2** (K_a = 4.7 × 10^4 M^{-1}) (Table 3). On the other hand, we observed strong binding of **9** under basic conditions (K_a > 10^6 M^{-1}). This result is ascribed to the electrostatic repulsion and attraction between the cationic cage and both positive and negative charges of the free terminals. In contrast to **9**, the affinities of the protected peptide **2** were not affected by pH conditions.

Next, we applied the electrostatic effect on the sequence-selective recognitions. We elucidated the electrostatic effect by examining the hexapeptides Ac-Ala-Trp-Trp-Ala-Gly-Xxx-NH_2. As discussed above, the Xxx6 residue of this peptide is out of the cage. Thus, residue Xxx6 was not expected to affect the conformation of the inclusion complex. Under acidic conditions, the association constant of **1** with the hexapeptide Ac-Ala-Trp-Trp-Ala-Gly-Lys-NH_2 (**10**), possessing cationic residue Lys, dramatically decreased. On the other hand, the anionic peptide Ac-Ala-Trp-Trp-Ala-Gly-Glu-NH_2 (**11**) showed higher affinity than the neutral peptide **8** under any pH conditions. This indicated that anionic and neutral peptides were bound by cage **1** more than 100-times stronger than cationic peptides.

Importance of Charge-Transfer Effect. Cage **1** could discriminate similar aromatic residues due to the difference in charge-transfer interaction between electron-rich aromatic residues and electron-deficient triazine parts of **1**. In fact, Ac-Ala-

Table 4. Association Constants of **1** with Peptides in Water

Peptides	K_a/M^{-1} a)	
	pH 4.8 (Acetate buffer)	pH 9.0 (Borate buffer)
Ac-Ala-**Trp**-**Trp**-NH_2 (**4**)	3.7 ($\pm$0.6) $\times$ 10^4	4.0 ($\pm$0.2) $\times$ 10^4
Ac-Ala-Tyr-Tyr-NH_2 (**12**)	6.8 ($\pm$1.2) $\times$ 10^3	$>10^5$

a) Measured by UV–vis titration at 20 °C in 5 mM buffer solution.

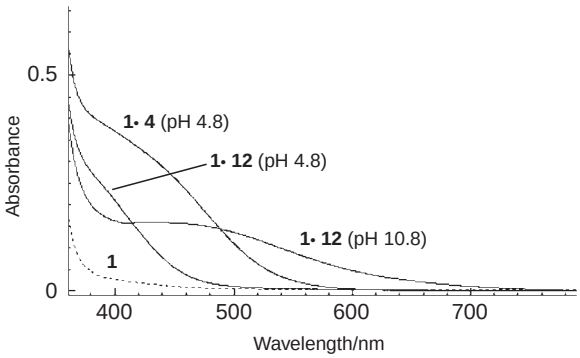

Fig. 4. UV spectra of **1**, **1·4** (pH 4.8), and **1·12** (pH 4.8 and 10.8) at 20 °C ([**1**], [**4**], and [**12**] = 3.0 mM in H_2O).

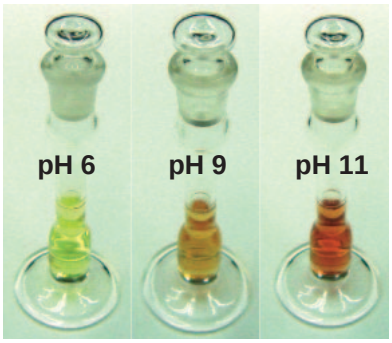

Fig. 5. Pictures of the **1·12** solution at several pH conditions ([**1**] and [**12**] = 3.0 mM in H_2O). The solution was adjusted from pH 6 to pH 11 using 100 mM NaOH.

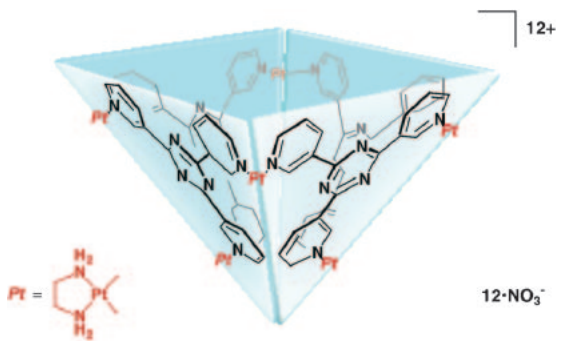

13

Scheme 2.

Trp-Trp-NH_2 (**4**) was bound about 5-fold stronger than Ac-Ala-Tyr-Tyr-NH_2 (**12**) in an acetate buffer solution (Table 4). This difference is attributed to the efficiency of charge-transfer interactions, because the charge-transfer absorption of complex **1·4** is more red-shifted than that of **1·12** (Fig. 4).

The binding of aromatic peptides having a Tyr residue was significantly enhanced under basic conditions. In a borate buffer solution (pH 9.0), the peptide **12** was bound about ten times as strongly as **4** (Table 4). Since the charge-transfer band of **1·12** under basic conditions was much more red-shifted than that under acidic conditions, the increment of the binding constant of **1·12** was ascribed to not only electrostatic attraction, but also to efficient charge-transfer interaction between the phenolate anion of Tyr residues and cage **1** (Fig. 4).

This behavior was applicable to the naked-eye recognition of colorless aromatic peptides. The Trp residues in peptides were detected from the colorization of the peptide solution upon addition of **1**. For example, a solution of the **1·4** complex showed an orange color at any pH. Interestingly, cage **1** could discriminate Trp and Tyr residues even in naked-eye recognition. While the solution of complex **1·12** showed a pale yellow color under acidic or neutral conditions, the solution color changed to red under basic conditions (Fig. 5). This color change corresponds to the change in UV spectra as shown in Fig. 4. On the other hand, Phe residues in peptides exhibited little color change in the presence of cage **1**. Namely, we could discriminate three aromatic residues, Trp, Tyr, and Phe, from solution colors when mixed with the coordination cage **1**.

Aromatic Peptide Recognition by Self-Assembled Bowl-Shaped Cavity. Similar to the cage-shaped host **1**, the self-assembled bowl-shaped host **13** also recognized aromatic peptides with high affinity (Scheme 2).[12] For example, **13** bound the hexapeptide Ac-Ala-Trp-Trp-Ala-Gly-Ser-NH_2 (**8**) more strongly than **1** (for **13·8**, $K_a = 1.3 \times 10^5\,M^{-1}$). Similar to **1**, **13** has electron-deficient triazine parts and a high cationic property (12+). Thus, **13** can recognize aromatic peptides with good selectivity. Since the open-shaped cavity of **13** can cover a large area, the bowl-shaped host **13** is expected to employ the pin-point recognition of a protein surface that often mediates protein–protein interactions.

Conclusion

In conclusion, we demonstrated that the self-assembled coordination cage **1** recognized aromatic peptide containing Trp residues with high selectivity and affinity. Cage **1** could discriminate even longer peptides (up to hexapeptides in the present work) by means of some interactions, steric, electrostatic, and charge-transfer, between cage **1** and peptides. Moreover, the selectivity of peptides containing charged residues or Tyr residues could be controlled by pH conditions due to the cationic property of the coordination cage (12+). We believe that the selectivity of aromatic peptides in this report will be applied to site-specific recognition of protein surfaces, because the bowl-shaped cage **13**, which is suitable for wrapping the protein surface, expects to show the same ability of peptide recognition.

Experimental

Materials. Organic solvents and reagents were purchased from TCI Co., Ltd., WAKO Pure Chemical Industries Ltd., and Aldrich Chemical Ltd. Deuterated solvents were acquired from Cambridge Isotope Laboratories, Inc. Fmoc amino acids and some reagents for peptide synthesis were purchased from Watanabe Chemical Industries Ltd. The platinum cage **1** was prepared following the procedure reported earlier.[11]

Peptide Synthesis. All peptides were synthesized by an automated peptide synthesizer (ABI 433A, Applied Biosystems) using standard Fmoc-based FastMoc coupling chemistry (0.1 mmol scale). Peptides were cleaved from the resin with TFA (10 mL) containing 5% (v/v) water and 5% (v/v) 1,2-ethanedithiol as a scavenger at room temperature for 3 h. Free peptides were washed from the resin with TFA (3 mL), followed by dichloromethane (5 mL), and then evaporated. To residues were added a large amount of Et_2O, and the precipitate was collected by filtration. Crude peptides were purified by reversed-phase HPLC on an Inertsil Peptides C18 (GL Sciences Inc.) semi-preparative column (20 mm × 250 mm) using aqueous 0.1% TFA and an acetonitrile gradient. The white powder of peptides was obtained by lyophilization. The characterization of peptides was carried out by ^{1}H NMR and MALDI-TOF mass (Voyager-DE STR, Applied Biosystems).

Synthesis of 13.[13] 2,4,6-Tri-3-pyridyl-1,3,5-triazine (0.20 mmol), $Pt(NO_3)_2$(en) (0.30 mmol), and 2-naphthoic acid (0.25 mmol) as a template were combined in H_2O (10 mL) and stirred for 6 days at 90 °C. After filtration, a small amount of nitric acid was added to the solution, the resulting slightly acidic solution was washed five times with chloroform, and then the solution was concentrated. A large amount of acetone was added to the concentrated solution to give a white precipitate. This precipitate was collected and washed with acetone. After drying, the white powder was dissolved in water, and then this solution was lyophilized (for complete evaporation of residual acetone).

UV–Vis Titration. A peptide was dissolved in water under sonication, and the solution was filtered by a disk-filter to remove trace amounts of insoluble impurities. The concentration of the peptide was determined by the absorption of Trp and Tyr residues.[14] The peptide solution (3.0 mL) was placed in a 1 cm quartz cell. The aqueous solution of cage **1** (5 mM) was added in portions via a microsyringe to the cell. All titrations were carried out at room temperature under a buffer solution (5 mM). Since cage **1** and the peptide itself have no absorption at 480 nm, the absorption appearing at 480 nm (or 440 nm for Ala-Tyr-Tyr) was monitored for the titration. The change in volume due to the addition of **1** was less than 3%. The association constant was calculated by a nonlinear curve-fitting procedure.[15]

NMR Spectroscopy. NMR spectra were recorded on a Bruker DRX-500 spectrometer at 300 K. TOCSY and NOESY were measured in phase-sensitive mode. Mixing times of TOCSY and NOESY were 80 and 300 ms, respectively. For water signal suppression, a WATERGATE solvent suppression scheme was applied to most NMR experiments. All spectra were processed using XWINNMR.

Supporting Information

NMR studies (Figures S1–S6) and UV-titrations (Figures S7–S24) are formatted in PDF files. This material is available free of charge on the web at: http://www.csj.jp/journals/bcsj/.

References

1 S. M. Albelda, C. A. Buck, *FASEB J.* **1990**, *4*, 2868; S. Jones, J. M. Thornton, *Proc. Natl. Acad. Sci. U.S.A.* **1996**, *93*, 13; W. E. Stites, *Chem. Rev.* **1997**, *97*, 1233.

2 M. W. Peczuh, A. D. Hamilton, *Chem. Rev.* **2000**, *100*, 2479.

3 S. S. Yoon, W. C. Still, *J. Am. Chem. Soc.* **1993**, *115*, 823; S. R. LaBrenz, J. W. Kelly, *J. Am. Chem. Soc.* **1995**, *117*, 1655; C.-T. Chen, H. Wagner, W. C. Still, *Science* **1998**, *279*, 851; M. A. Hossain, H.-J. Schneider, *J. Am. Chem. Soc.* **1998**, *120*, 11208; K. B. Jensen, T. M. Braxmeier, M. Demarcus, J. G. Frey, J. D. Kilburn, *Chem. Eur. J.* **2002**, *8*, 1300; K. Tsubaki, T. Kusumoto, N. Hayashi, M. Nuruzzarman, K. Fuji, *Org. Lett.* **2002**, *4*, 2313; C. Schmuck, L. Geiger, *J. Am. Chem. Soc.* **2004**, *126*, 8898; R. Zadmard, M. Arendt, T. Schrader, *J. Am. Chem. Soc.* **2004**, *126*, 7752; A. Ojida, Y. Miyahara, T. Kohira, I. Hamachi, *Biopolymers* **2004**, *76*, 177; M. Kruppa, C. Mandl, S. Miltschitzky, B. König, *J. Am. Chem. Soc.* **2005**, *127*, 3362; M. Fokkens, T. Schrader, F.-G. Klärner, *J. Am. Chem. Soc.* **2005**, *127*, 14415.

4 J. S. Albert, M. S. Goodman, A. D. Hamilton, *J. Am. Chem. Soc.* **1995**, *117*, 1143; M. W. Peczuh, A. D. Hamilton, J. Sánchez-Quesada, J. Mendoza, T. Haack, E. Giralt, *J. Am. Chem. Soc.* **1997**, *119*, 9327; Y. Hamuro, M. C. Calama, H. S. Park, A. D. Hamilton, *Angew. Chem., Int. Ed. Engl.* **1997**, *36*, 2680; H. S. Park, Q. Lin, A. D. Hamilton, *J. Am. Chem. Soc.* **1999**, *121*, 8.

5 A. A. Bogan, K. S. Thorn, *J. Mol. Biol.* **1998**, *280*, 1.

6 E. A. Padlan, *Mol. Immunol.* **1994**, *31*, 169; K. Tsumoto, K. Ogasahara, Y. Ueda, K. Watanabe, K. Yutani, I. Kumagai, *J. Biol. Chem.* **1995**, *270*, 18551.

7 R. Ueoka, Y. Matsumoto, K. Harada, H. Akahoshi, Y. Ihara, Y. Kato, *J. Am. Chem. Soc.* **1992**, *114*, 8339; M. Maletic, H. Wennemers, D. Q. McDonald, R. Breslow, W. C. Still, *Angew. Chem., Int. Ed. Engl.* **1996**, *35*, 1490; R. Breslow, Z. Yang, R. Ching, G. Trojandt, F. Odobel, *J. Am. Chem. Soc.* **1998**, *120*, 3536; D. Wilson, L. Perlson, R. Breslow, *Bioorg. Med. Chem.* **2003**, *11*, 2649.

8 M. Fujita, *Chem. Soc. Rev.* **1998**, *27*, 417; M. Fujita, K. Umemoto, M. Yoshizawa, N. Fujita, T. Kusukawa, K. Biradha, *Chem. Commun.* **2001**, 509; M. Fujita, M. Tominaga, A. Hori, B. Therrien, *Acc. Chem. Res.* **2005**, *38*, 371.

9 T. Kusukawa, M. Fujita, *J. Am. Chem. Soc.* **2002**, *124*, 13576; M. Yoshizawa, M. Tamura, M. Fujita, *J. Am. Chem. Soc.* **2004**, *126*, 6846; M. Yoshizawa, J. Nakagawa, K. Kumazawa, M. Nagao, M. Kawano, T. Ozeki, M. Fujita, *Angew. Chem., Int. Ed.* **2005**, *44*, 1810.

10 S. Tashiro, M. Tominaga, M. Kawano, B. Therrien, T. Ozeki, M. Fujita, *J. Am. Chem. Soc.* **2005**, *127*, 4546.

11 F. Ibukuro, T. Kusukawa, M. Fujita, *J. Am. Chem. Soc.* **1998**, *120*, 8561.

12 S.-Y. Yu, T. Kusukawa, K. Biradha, M. Fujita, *J. Am. Chem. Soc.* **2000**, *122*, 2665; M. Yoshizawa, Y. Takeyama, T. Kusukawa, M. Fujita, *Angew. Chem., Int. Ed.* **2002**, *41*, 1347.

13 S. Tashiro, M. Tominaga, Y. Yamaguchi, K. Kato, M. Fujita, *Angew. Chem., Int. Ed.* **2006**, *45*, 241.

14 J. F. Brandts, L. J. Kaplan, *Biochemistry* **1973**, *12*, 2011.

15 UV–vis titration curves of peptides are described in Supporting Information.